

## Cathodic Hydrogen Evolution Reaction on Gold Catalyzed by Proton-Carriers

Raluca Crețu, Andrea Kellenberger, Mihai Medeleanu, Nicolae Vaszilcsin\*

Universitatea Politehnica Timișoara, Faculty of Industrial Chemistry and Environmental Engineering,  
300006 Piata Victoriei 2, Timișoara, Romania

\*E-mail: [nicolae.vaszilcsin@upt.ro](mailto:nicolae.vaszilcsin@upt.ro)

Received: 6 March 2014 / Accepted: 3 April 2014 / Published: 19 May 2014

---

Several amines with aromatic and aliphatic substituents have been investigated as catalysts in the solution for the hydrogen evolution reaction, based on their ability to increase the concentration of protons in the electric double layer at the interface, by transporting protons from the bulk solution to the cathode surface. The highest electrocatalytic activity, expressed by the activation energy for hydrogen evolution reaction has been obtained for methylamine, 4-chloroaniline and aniline. In this series, the catalytic activity is primarily influenced by the molecular coverage area, which determines the number of protonated molecules that can adsorb on the cathode surface. The second factor that affects catalytic activity is the magnitude of the dipole moment, which determines a preferential orientation of the protonated molecule at the interface. As a consequence, methylamine shows the highest catalytic activity due to its low coverage area and 4-chloroaniline has a stronger effect than aniline due to its larger dipole moment induced by the electron-withdrawing inductive effect of chlorine. A mechanism for hydrogen evolution reaction in the presence of amines has been proposed, where both hydronium and ammonium ions are involved in the charge transfer process.

---

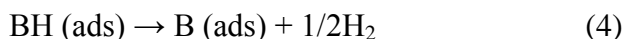
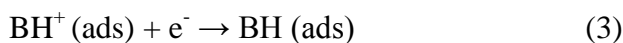
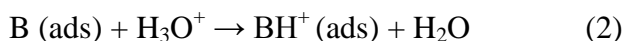
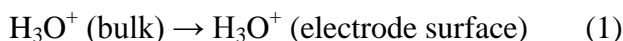
**Keywords:** Hydrogen evolution reaction, proton carriers, Tafel plots, Arrhenius plots, Charge transfer coefficient

### 1. INTRODUCTION

The research concerning the enhancement of hydrogen evolution reaction continues to maintain its actuality due to the remarkable interest for hydrogen production based on electrochemical procedures [1-8] as an alternative to the processes using fossil row materials in which appreciable amounts of carbon dioxide are produced. Until now, several studies carried out in this respect have led to the development of some cathodes with catalytic effect for hydrogen evolution reaction (HER) [9]. On the one hand, an increase of the hydrogen atoms generation (Volmer step) was achieved, in

particular using some noble metals as platinum or palladium [10,11], and on the other hand, the hydrogen recombination (Tafel or Heyrovsky step) has been stimulated by some metals like nickel or cobalt [12-15]. Furthermore, bifunctional catalysts which stimulate both the charge transfer and chemical or electrochemical recombination processes have been developed [16-18].

The catalytic effect on HER can be manifested as well in the electrolyte solution from the proximity of the electrode. In a strong acid medium, using mercury electrode, the catalytic effect of the organic bases on HER has been reported since the 30's [19]. A mechanism in which the overall process takes place in four successive steps has been proposed by Stackelberg et al. (1-4) [20-22]. The authors have assumed that at low current densities the charge transfer (3) is a slow step, while at higher current densities the protonation of the organic base (2) become the slow one:



The influence of organic bases, like aromatic amines, in HER has been studied for over a decade almost exclusively on dropping mercury electrode mainly due to the fact that the surface of this type of electrode is perfectly reproducible, but also due to the high overpotentials for hydrogen evolution at which catalytic effect is more pronounced [23,24].

As it is well known, metals with high overpotential for HER do not show a practical importance as cathodes used in hydrogen production by water electrolysis. Consequently, for a long time practical application of the catalytic effect of organic bases in HER has not been taken into consideration. Recently, this effect has been also studied on metals with lower HER overpotential [25,26].

The HER on gold electrode occurs at moderate overpotential so the influence of the amines structure on the catalytic properties can be easily highlighted evidenced. It is also possible to use gold as dopant for platinum materials to realize bifunctional cathodes with catalytic activity for both charge transfer reaction and chemical or electrochemical desorption processes. According to the *volcano curve* for HER, the strength of metal-hydrogen bond for Au is very close to that of iron group metals [27] and therefore gold should provide a similar catalytic effect on the recombination of hydrogen atoms. Thereby, the development of bifunctional electrocatalysts with activity in strongly acidic medium for hydrogen evolution is possible.

The aim of this paper is to present a detailed study on the catalytic effect of methylamine (MA), aniline (A) and 4-chloroaniline (CIA) towards HER on gold electrode. These amines have been selected following some preliminary measurements, in which they have exhibited the best catalytic effect.

## 2. EXPERIMENTAL

Experimental measurements have been carried out in  $0.5 \text{ mol L}^{-1} \text{ H}_2\text{SO}_4$  supporting electrolyte solution at different concentrations of the amines of  $10^{-6}$ ,  $10^{-5}$ ,  $10^{-4}$  and  $10^{-3} \text{ mol L}^{-1}$  aniline, 4-chloroaniline and methylamine, respectively. The effect of temperature has been studied at four different temperatures (298, 308, 318 and 328 K), using a Thermo Scientific DC 10 thermostat, having an accuracy of  $\pm 0.1 \text{ K}$ .

Linear voltammograms have been recorded with a PAR 2273 potentiostat – galvanostat equipped with specific modules and software (Power Suite for voltammetric data).

A typical three electrode/one compartment electrochemical cell, using gold as working electrode ( $A = 0.02 \text{ cm}^2$ ,  $\phi = 1.6 \text{ mm}$ ), a platinum sieve as counter electrode and Ag/AgCl (sat) electrode as reference, has been used. Before each electrochemical experiment the working electrode was polished using a Struers spray with polycrystalline diamond (particle size  $1 \mu\text{m}$ ), further washed with distilled water, and finally cleaned with distilled water in an ultrasonic bath for 3 minutes.

To determine the reversible potential for HER a galvanostatic step was applied to the working electrode as described in more detail elsewhere (galvanic step of  $250 \text{ mA cm}^{-2}$  was applied for 30 s) [26]. The values of the reversible potential obtained from the potential – time curves at different temperatures (Fig. 1) are presented in Table 1. HER overpotentials were calculated as difference between the actual (measured) potential and reversible one.

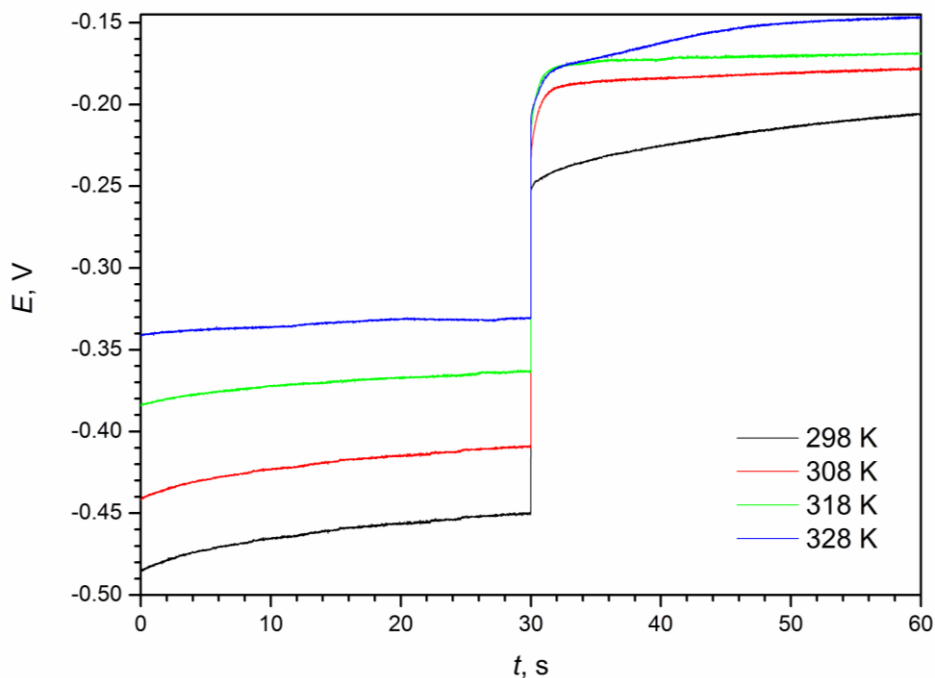


**Figure 1.** Galvanostatic step on gold electrode in  $0.5 \text{ mol L}^{-1} \text{ H}_2\text{SO}_4$  at 308 K.

**Table 1.** Experimental values of reversible potential, at different temperatures.

T [K]	298	308	318	328
$E_{\text{rev}}$ [V]	-0.203	-0.179	-0.169	-0.147

Based on Tafel plots  $\eta = f(\log i)$ , where  $\eta$  represents overpotential, in V and  $i$  – current density, in  $\text{A m}^{-2}$ , the kinetic parameters have been calculated. Also, considering the linear dependence  $\lg |i_0| = f(T^{-1})$  and using Arrhenius equation, the apparent activation energy has been determined [26].

Quantum estimation was carried out in order to determine dipole moments and frontier orbitals energy (HOMO – highest occupied molecular orbital, LUMO - lowest unoccupied molecular orbital) for the protonated. Therefore, GAUSSIAN09 package was used based on density functional B3LYP/6-311 + G variant (d, p) method [28]. In addition, the van der Waals molecular parameters (volume, surface area and the molecular ellipsoid circumscribed semi-axes) were calculated [29]. Based on ellipsoid parameters the molecular covering area normalized on the dipole moment has been calculated.

Reagents used were: sulfuric acid p.a. > 95 – 97 % (Merck), ammonium sulphate p.a. > 99.5% (Fluka), aniline  $\geq 99.5$  % (Merck), 3 – chloroaniline  $\geq 99\%$  (Merck), 4 – chloroaniline  $\geq 99\%$  (Merck), 2-biphenylamine  $\geq 98\%$  (Merck), DL-1-phenylethylamine  $\geq 98\%$  (Merck), and methylamine > 95 % (Aldrich).

### 3. RESULTS AND DISCUSSION

Preliminarily, the catalytic effect on HER of some amines like methylamine, aniline, N-methylaniline, 3-chloroaniline, 4-chloroaniline, 2-biphenylamine, DL-1-phenylethylamine, as well as ammonium sulphate, on Au electrode in  $0.5 \text{ mol L}^{-1} \text{ H}_2\text{SO}_4$  solution, has been investigated by linear voltammetry.

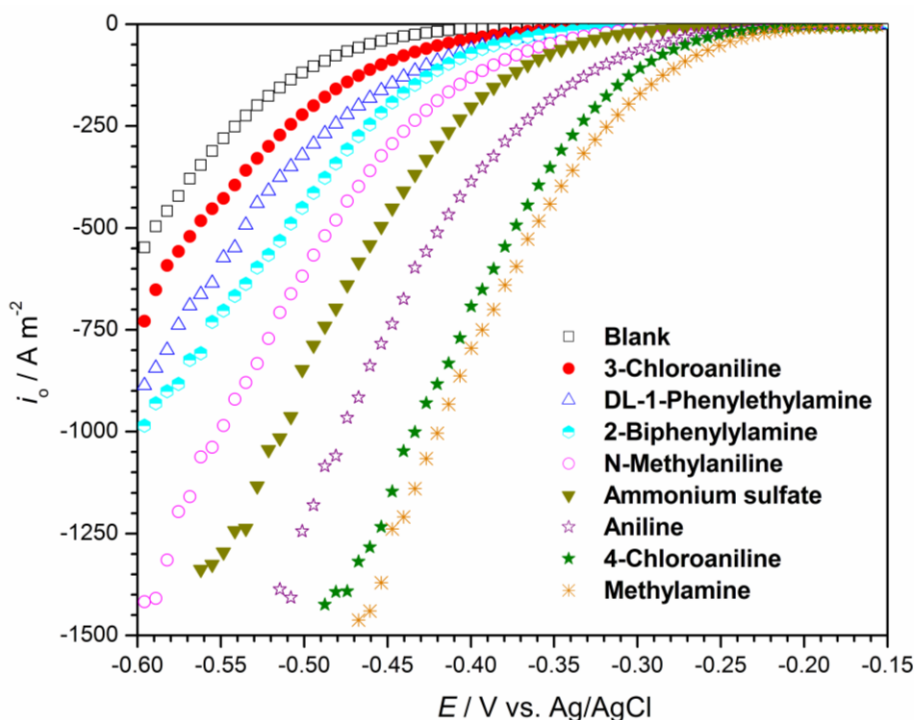


**Figure 2.** Linear voltammograms on smooth gold electrode in  $0.5 \text{ mol L}^{-1} \text{ H}_2\text{SO}_4$  solution at  $25^\circ\text{C}$ , concentration of amines:  $10^{-3} \text{ mol L}^{-1}$ , scan rate:  $10 \text{ mV s}^{-1}$ .

In order to study the kinetics of HER methylamine, aniline and 4-chloroaniline have been chosen as proton carriers, because their effect is more significant, as it is shown in Figure 2. The reduction of hydrogen overpotential in the presence of  $10^{-3}$  mol L<sup>-1</sup> of the above mentioned amines in 0.5 mol L<sup>-1</sup> H<sub>2</sub>SO<sub>4</sub>, at 25°C, is considerable, reaching 0.23 V, 0.22 V and 0.17 V for methylamine, 4-chloroaniline and aniline, versus blank solution, at 500 A m<sup>-2</sup> current density.

On the other hand, the molecular structural differences between these three amines are pronounced enough to offer the possibility to accomplish some correlations between catalytic properties and their molecular parameters.

To determine the kinetic parameters for HER, the Tafel plots were recorded in the absence and presence of amines at different temperatures that allows the evaluation of both exchange current density  $i_0$  and cathodic transfer coefficient  $1-\alpha$  as well as of the activation energy  $E_a$ .

L.A. Khanova and L.I. Krishtalik have proved that on gold, in sulphuric acid solution, Tafel plots present two distinct slopes. The smaller, obtained at low overpotential, corresponds to the HER controlled by desorption of the hydrogen atoms, while the larger one is due to the mechanism in which the charge transfer is slow step of the cathodic process [30]. Therefore, in order to determine kinetic parameters that characterize the charge transfer, Tafel slopes were plotted for a limiting domain of high overpotentials.

Figure 3 and Figure 4 present the Tafel plots obtained in 0.5 mol L<sup>-1</sup> H<sub>2</sub>SO<sub>4</sub> solution without and with  $10^{-6}$  mol L<sup>-1</sup> protonated amines at different temperatures (298 K, 308 K, 318 K and 328 K), respectively with  $10^{-3}$  mol L<sup>-1</sup> protonated amines.

The transfer coefficient  $1-\alpha$  was calculated using the Butler-Volmer equation for the limiting case of high overpotential, from the Tafel slope  $b$  given by relationship (5):

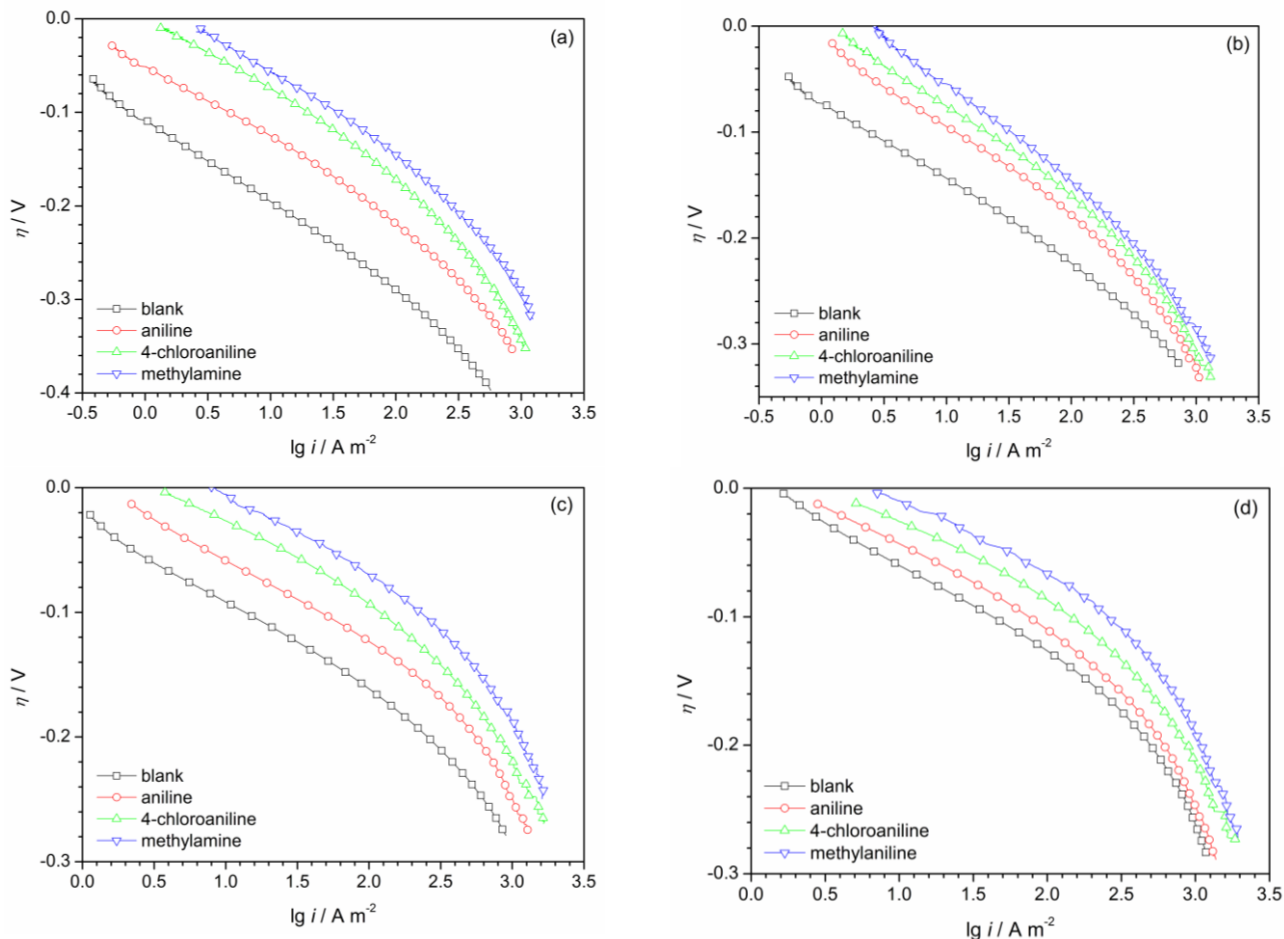
$$b = -\frac{2.303RT}{(1-\alpha)F} \quad (5)$$

where  $R$  is the gas constant (8.31451 J mol<sup>-1</sup> K<sup>-1</sup>),  $T$  - thermodynamic temperature (K),  $F$  - Faraday's number (96,485 C mol<sup>-1</sup>).

The exchange currents  $i_0$  were evaluated from Tafel slope intersection with the abscissa ( $\lg |i_0|$ ). The obtained values of the kinetic parameters for the three investigated amines as a function of concentration and temperature are shown in Table 2.

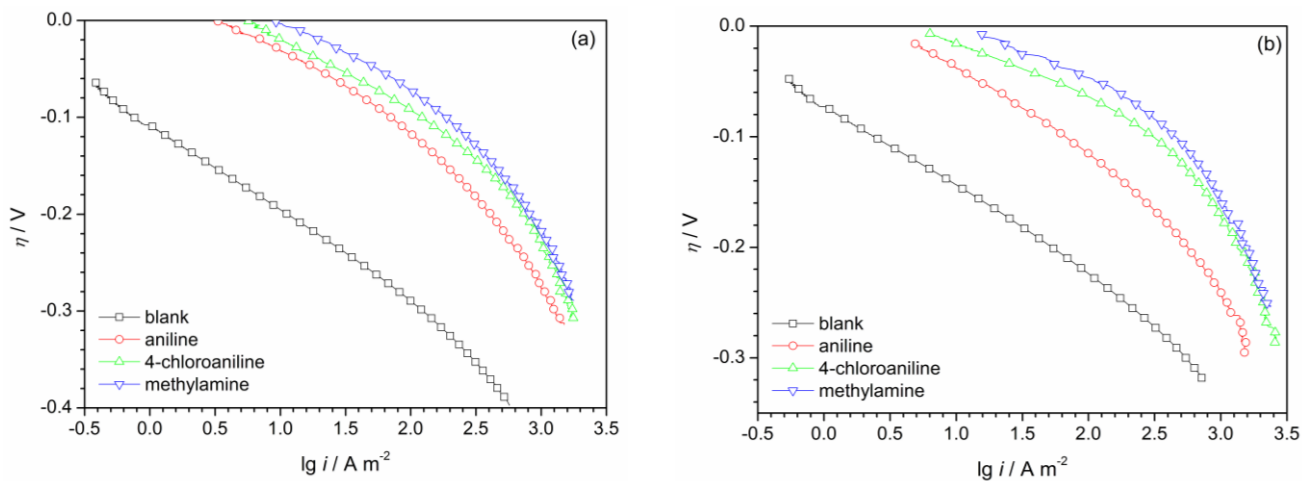
According to the data presented in Table 2, it can be observed that in the presence of amines, the charge transfer coefficient  $1-\alpha$  decreases in all of experiments. Overall, the values of the charge transfer coefficient  $1-\alpha$  in the presence of amines increases in the series MAH<sup>+</sup> > ClAH<sup>+</sup> > AH<sup>+</sup>. To explain this phenomenon it is necessary to take into account that the charge transfer coefficient  $1-\alpha$  represents a measure of the activated complex coordinates at the metal – electrolyte solution interface.

The lower the value of  $1-\alpha$ , the farther is the reaction plane from the metal surface. The significant shift of  $1-\alpha$  to lower values may be assigned to the fact that more voluminous particles than hydronium ions are involved in the charge transfer reaction, like alkylammonium or arylammonium cations, which for steric reasons can not approach as close to the metal surface as hydronium ions. In the electric field from the metal-solution interface, the dipole molecules of protonated amines show a net orientation with the positive pole toward the metal surface. For similar molecular volumes, the higher the dipole moment, the closer is the inner Helmholtz plane to the metal surface.



**Figure 3.** Tafel plots on Au electrode in 0.5 mol L<sup>-1</sup> H<sub>2</sub>SO<sub>4</sub> solution without and with 10<sup>-6</sup> mol L<sup>-1</sup> protonated amines at 298 (a), 308 (b), 318 (c) and 328 (d) K.

Likewise, the molecules having larger volume, due to the thermal motion, are easily withdraw from the metal surface. Consequently, at room temperatures, besides the hydronium discharge reaction (16), a parallel ammonium ions discharge reaction may occurs (13).



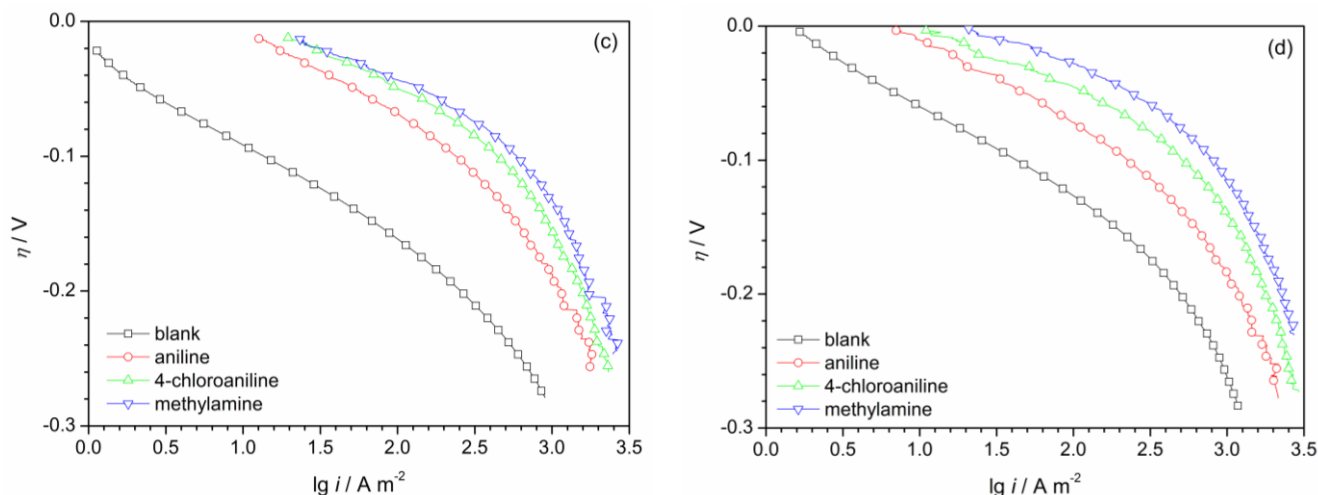


**Figure 4.** Tafel plots on Au electrode in 0.5 mol L<sup>-1</sup> H<sub>2</sub>SO<sub>4</sub> solution without and with 10<sup>-3</sup> mol L<sup>-1</sup> protonated amines at 298 (a), 308 (b), 318 (c) and 328 (d) K.

**Table 2.** Experimental values of Tafel slope, transfer coefficient 1- $\alpha$  and exchange current  $i_0$ , in the absence and presence of amines.

$c$ [mol L <sup>-1</sup> ]	$T$ [K]	$-b$ [mV dec <sup>-1</sup> ]			$1-\alpha$			$i_0$ [A m <sup>-2</sup> ]		
		AH <sup>+</sup>	CIAH <sup>+</sup>	MAH <sup>+</sup>	AH <sup>+</sup>	CIAH <sup>+</sup>	MAH <sup>+</sup>	CIAH <sup>+</sup>	MAH <sup>+</sup>	
0	298		114		0.52			0.29		
	308		121		0.51			1.75		
	318		130		0.49			7.63		
	328		141		0.46			17.97		
10 <sup>-6</sup>	298	123	135	141	0.48	0.44	0.42	1.71	5.27	10.84
	308	130	150	151	0.47	0.41	0.40	4.67	10.59	13.30
	318	154	161	164	0.41	0.39	0.38	26.50	43.74	71.45
	328	162	172	183	0.40	0.38	0.36	33.79	58.59	91.17
10 <sup>-5</sup>	298	123	139	153	0.48	0.43	0.39	3.48	11.42	17.86
	308	134	144	163	0.46	0.42	0.39	6.54	29.03	54.37
	318	154	169	187	0.41	0.37	0.34	32.89	76.76	133.08
	328	180	185	201	0.36	0.35	0.32	50.12	94.95	146.09
10 <sup>-4</sup>	298	133	145	159	0.44	0.41	0.37	8.00	20.53	33.31
	308	142	167	171	0.43	0.37	0.36	11.25	66.35	94.35
	318	161	184	199	0.39	0.34	0.32	51.30	116.70	160.93
	328	183	193	211	0.36	0.34	0.31	60.04	130.96	192.95
10 <sup>-3</sup>	298	148	165	181	0.40	0.36	0.33	17.78	44.06	64.10
	308	155	173	185	0.39	0.35	0.33	27.74	98.22	141.29
	318	171	196	205	0.37	0.32	0.31	75.74	155.28	214.23
	328	186	210	216	0.35	0.31	0.30	94.41	207.13	296.73

AH<sup>+</sup>, CIAH<sup>+</sup> and MAH<sup>+</sup> represent the protonated forms of A, CIA and respectively MA.

At increased temperatures, the rate of ammonium ions hydrolysis increases, more exactly the global process, including protonated amines diffusion, hydrolysis, diffusion of neutral amines into the solution and their protonation, is enhanced, in such a way that the contribution of the cathodic discharge reaction of ammonium ions is diminished (13). The temperature rise, i.e. the enhancement of the thermal motion, will lead to an increase of the distance up to which ammonium and/or hydronium ions may approach the metal surface. That is a cause of the transfer coefficient  $1-\alpha$  reduction.

According to the Butler – Volmer equation, a low charge transfer coefficient  $1-\alpha$  is unfavorable for HER kinetics, but as it will be seen below this effect may be offset and exceeded by the consistent increase of the exchange current density  $i_0$ . The protonated amines have a much stronger influence on the exchange current density  $i_0$  than on the transfer coefficient because their adsorption on the cathode surface leads to a higher concentration of proton carriers which can be discharged.

Moreover, the protonated amines can be hydrolyzed in the double layer at the metal – solution interface, since in this region, as a result of HER, the solution pH increases up to values at which the hydrolysis of proton carriers become possible. It is well known that exchange current density  $i_0$  is directly proportional to the concentration of electroactive ions at the interface, according to relation (6) [31].

$$i_0 = F \cdot c_{\text{Ox}} \cdot k_c \exp\left(-\frac{E_a}{RT}\right) \quad (6)$$

where  $c_{\text{Ox}}$  is the concentration of the electroactive particles,  $k_c$  – rate constant of the cathodic process,  $E_a$  – activation energy.

In the absence of protonated amines, the exchange current density will be determined only by the hydronium ions concentration, provided that the rate determining step is the charge transfer:

$$i_{0(b)} = F \cdot c_{\text{H}_3\text{O}^+(b)} \cdot k_{c(b)} \exp\left(-\frac{E_{a(b)}}{RT}\right) \quad (7)$$

where  $i_{0(b)}$  is the exchange current density,  $c_{\text{H}_3\text{O}^+(b)}$  - hydronium concentration,  $k_{c(b)}$  - rate constant of cathodic reduction of hydronium ions,  $E_{a(b)}$  – activation energy (all referred to the blank solution).

In the presence of protonated amines, the concentration of hydronium ions increases with  $c_{\text{H}_3\text{O}^+(a)}$  due to the hydrolysis of ammonium ions. It must be taken into account that the discharge of ammonium ions may also occur on the cathode. In this case, the global exchange current density will be:

$$i_0 = F \cdot \left[ c_{\text{H}_3\text{O}^+(b)} + c_{\text{H}_3\text{O}^+(a)} \right] \cdot k_{c(\text{H}_3\text{O}^+)} \exp\left(-\frac{E_{a(\text{H}_3\text{O}^+)}}{RT}\right) + F \cdot c_{\text{RH}^+} \cdot k_{\text{RH}^+} \exp\left(-\frac{E_{a(\text{RH}^+)}}{RT}\right) \quad (8)$$

where  $\text{RH}^+$  represents the protonated forms of the studied amines  $\text{AH}^+$ ,  $\text{ClAH}^+$  and respectively  $\text{MAH}^+$ .

According to literature data, cathodic surface coverage with these species is high even at low concentrations, reason for which the exchange current density increases significantly in the presence of amines. Since it is difficult to separate the amines contribution to the increase of the hydronium ion concentration, a global relationship can be used:



$$i_o = F \cdot c_{\text{H}_3\text{O}^+}^* \cdot k_c^* \exp\left(-\frac{E_a^*}{RT}\right) \tag{9}$$

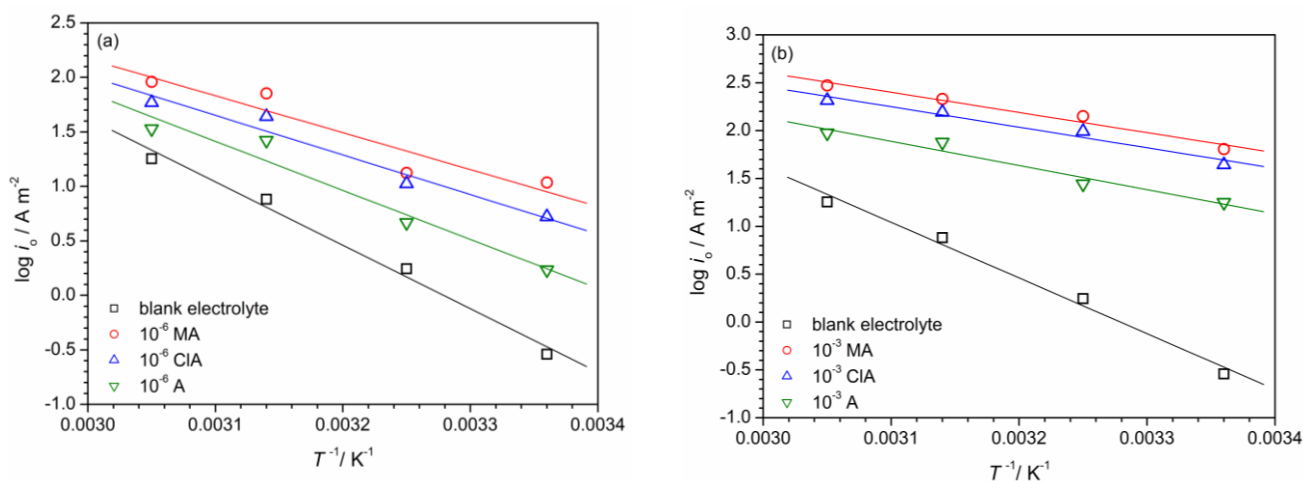
where  $c_{\text{H}_3\text{O}^+}^*$ ,  $k_c^*$  and  $E_a^*$  represent apparent values. Relation (9) allows to calculate the apparent activation energy, from the slope of the dependence  $\lg i_o = f(T^{-1})$  according to relationship (10) [32].

Figure 5 shows the Arrhenius plots both in the absence and in the presence of amines at a concentration of  $10^{-6} \text{ mol L}^{-1}$ , respectively  $10^{-3} \text{ mol L}^{-1}$ .

$$E_a = -2.303R \frac{\partial(\lg i_o)}{\partial(T^{-1})} \tag{10}$$

The addition of aniline to  $\text{H}_2\text{SO}_4$  solution leads to a reduction of the apparent activation energy from  $112 \text{ kJ mol}^{-1}$  (value obtained in blank solution) to  $86 \text{ kJ mol}^{-1}$  and  $48 \text{ kJ mol}^{-1}$ , for the solution with  $10^{-6} \text{ mol L}^{-1}$ , respectively  $10^{-3} \text{ mol L}^{-1}$  aniline. Likewise, for the other two amines, the value of the activation energy decreases to  $70 \text{ kJ mol}^{-1}$  and  $41 \text{ kJ mol}^{-1}$  at a concentration of  $10^{-6} \text{ mol L}^{-1}$ , respectively  $10^{-3} \text{ mol L}^{-1}$  4-chloroaniline, and to  $65 \text{ kJ mol}^{-1}$  and  $41 \text{ kJ mol}^{-1}$  at a concentration of  $10^{-6} \text{ mol L}^{-1}$ , respectively  $10^{-3} \text{ mol L}^{-1}$  methylamine.

It should be noted that in the strong acid media, used as electrolyte solution, the studied amines are completely ionized, taking into account that their acidity constants are:  $K_a = 2.51 \cdot 10^{-5}$  for aniline [33],  $K_a = 7.08 \cdot 10^{-5}$  for 4-chloroaniline [34] respectively  $K_a = 2.29 \cdot 10^{-11}$  for methylamine [33]. Accordingly, quantum estimations were carried out just for protonated amines.



**Figure 5.** Arrhenius plots for HER in  $0.5 \text{ mol L}^{-1} \text{ H}_2\text{SO}_4$  solution in the absence and in the presence of MA, CIA and A at concentrations of  $10^{-6} \text{ mol L}^{-1}$  (a) and respectively  $10^{-3} \text{ mol L}^{-1}$  (b).

The catalytic effect of the amines depends on their molecular characteristics. Some of the molecular parameters have been determined by quantum calculations and are presented in Table 3.

Molecular parameters which determine the proton carrier character are the dipole moment and coverage area. Taking into account that the molecules are preferentially oriented with the dipole moment normal on the metal surface, the last parameter can be assimilated with the maximum

molecular section area perpendicular on dipole moment. The guideline of the dipole moment in the amines molecule is given in Figure 6.

**Table 3.** Molecular parameters of protonated amines.

Compound	No of atoms	Molecular volume [ $\text{\AA}^3$ ]	Dipole moment [D]	Molecular coverage area [ $\text{\AA}^2$ ]	HOMO [eV]	LUMO [eV]
Anilinium, $\text{AH}^+$	15	95.3	7.12	30.9	-11.6	-5.3
4-Chloranilinium, $\text{ClAH}^+$	15	108.6	12.31	30.9	-11.1	-5.4
Methyl-ammonium, $\text{MAH}^+$	8	36.1	2.22	21.5	-17.2	-5.9

Among the studied protonated amines, the coverage area of  $\text{MAH}^+$  ( $21.5 \text{ \AA}^2$ ) is smaller than that of  $\text{AH}^+$  ( $30.9 \text{ \AA}^2$ ) or  $\text{ClAH}^+$  ( $30.9 \text{ \AA}^2$ ), and therefore a much higher number of  $\text{MAH}^+$  molecules can be adsorbed on the cathode surface, which ensures a higher concentration of hydronium ions at the interface, and consequently a higher exchange current density (see Table 2).

On the other hand,  $\text{AH}^+$  and  $\text{ClAH}^+$  coverage areas are very close, but the molecular dipole moments differ (7.12 D, respectively 12.31 D), because Cl atom has an electron-withdrawing inductive effect which produces a higher charge separation in  $\text{ClAH}^+$  than in  $\text{AH}^+$  and as a consequence  $\text{ClAH}^+$  dipole moment is higher than of  $\text{AH}^+$  one. It means that the orientation of  $\text{ClAH}^+$  dipoles on the electrode surface will be more ordered than of  $\text{AH}^+$  dipoles and in these circumstances a larger number of  $\text{ClAH}^+$  molecules will be able to adsorb on the electrode surface, thus ensuring a higher concentration of the electroactive particles and a higher exchange current density, as it can be seen in Table 2.

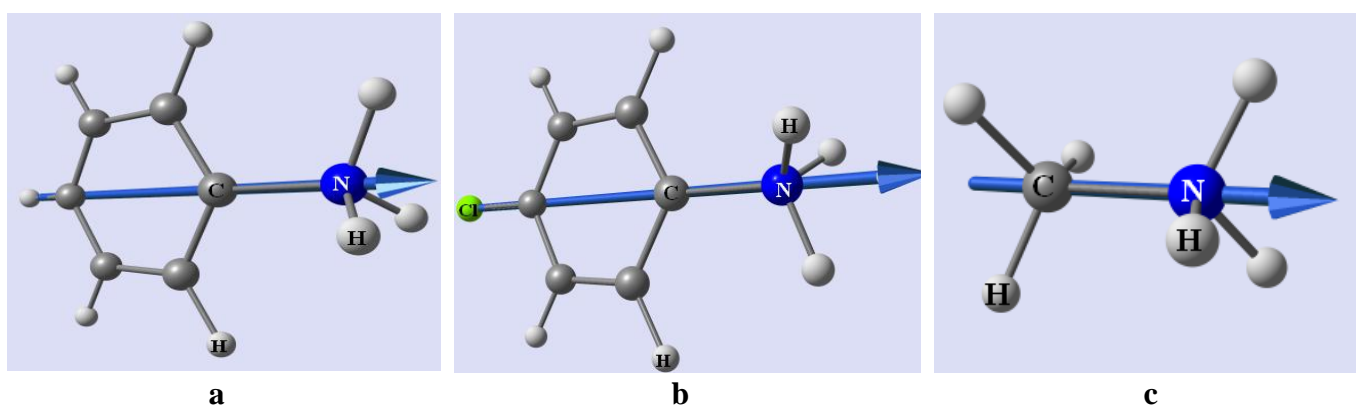
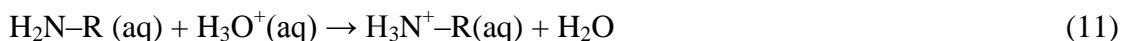


**Figure 6.** Molecular dipole moment (arrow) of protonated amines: a -  $\text{AH}^+$ ; b -  $\text{ClAH}^+$ , c -  $\text{MAH}^+$ .

Energy level of HOMO characterizes the ability of chemical entities to interact as electron donor, while energy level of LUMO is a descriptor of the electron acceptor properties. Consequently, in case of ammonium ions LUMO level will be a measure of the adsorption ability on gold cathode. As the LUMO energy values of  $\text{AH}^+$ ,  $\text{ClAH}^+$  and  $\text{MAH}^+$  are very close, this descriptor can not be used in order to characterize rigorously adsorption properties of protonated amines.

The results presented above justify a more detailed mechanism derived from that proposed by Stackelberg et al. [20-22], as follows:

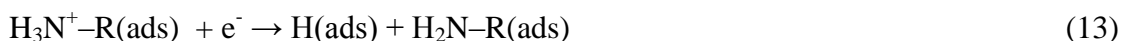
Ammonium ions (methyl-ammonium, phenylammonium and 4-chlorophenylammonium) are formed as a result of amines protonation in the bulk of solution:



In the electric field between the electrodes, ammonium ions migrate towards cathode, where they adsorb on the gold surface, with the nitrogen atoms oriented to the metal surface, according to the dipole moment, that is in a favorable position for charge transfer process:



Thereby, at Au-electrolyte solution interface, a high concentration of ammonium ions is reached. Taking into account that H-N bond energy in ammonium ions is lower than H-O bond in hydronium ions, it can be appreciated that at low current densities, where HER overpotential is not too large, the charge transfer occurs according to the reaction:



The recombination step of HER could occur chemically (Tafel step):



or electrochemically (Heyrovsky step):



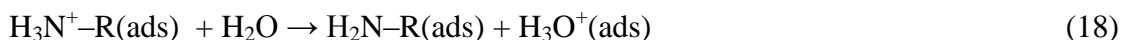
At higher current densities (elevated overpotential), hydronium ions discharge becomes possible:



followed by Tafel (chemical) or Heyrovsky (electrochemical) desorption:



The hydronium ions discharge has as a consequence a local pH increase of the solution adjacent to the cathode up to values that allow hydrolysis of ammonium ions:



This reaction helps to keep the concentration of hydronium ions at high values. The neutral amines diffuse into the bulk solution where the re-protonation reaction (11) occurs.

#### 4. CONCLUSIONS

The catalytic effect of several protonated amines on HER was compared using the kinetic parameters that characterize the electrode process. Exchange current density  $i_0$  and charge transfer coefficient  $1-\alpha$  were determined by the Tafel slope method, while the activation energy  $E_a$  was evaluated from Arrhenius plots. In the absence of amines, at standard temperature, the value of exchange current is small ( $0.22 \text{ A m}^{-2}$ ), but it increases substantially in the presence of amines, even 100 times, in the case of  $\text{ClAH}^+$  and about 175 times in the presence of  $\text{MAH}^+$ , both at a concentration of  $10^{-3} \text{ mol L}^{-1}$  in  $0.5 \text{ mol L}^{-1} \text{ H}_2\text{SO}_4$  solution. The influence of the above amines on the charge transfer coefficient  $1-\alpha$  is intricate in the circumstances in which this quantity is treated as a measure of the activated complex coordinate at the metal - electrolyte solution interface. The presence of amines

causes a decrease of the charge transfer coefficient, unfavorable for electrode kinetics. But this effect is offset by the significant increase of the exchange current density. The opposite effects of the exchange current density and charge transfer coefficient are brought together by the activation energy. Since in the charge transfer process two chemical species (hydronium and ammonium ions) are involved, an apparent value of the activation energy has been obtained. The diminution of this quantity when amines are added in solution is less pronounced than the increase of the exchange current density because of the adverse influence of the charge transfer coefficient. For example, in the case of 0.5 mol L<sup>-1</sup> H<sub>2</sub>SO<sub>4</sub> solution with protonated methylamine the activation energy is about 3 times less than in the case of the same solution without amine, but the exchange current density is almost 200 times higher.

The catalytic effects of the proton carriers can be linked to the molecular characteristics of protonated amines, among which dipole moment, molecular volume and coverage area have an important influence.

Based on these results a modified mechanism of HER from Stackelberg's one has been proposed, in which a direct discharge of hydronium ions was taken into account. In such a way, the protonation of amines can not be the rate determining step of the cathodic process, even at high overpotential, contrary to the Stackelberg's mechanism.

#### ACKNOWLEDGEMENT

This work was partially supported by the projects POSDRU 137070 *ATTRACTING* and BS ERA.NET 31/2011 *HYSULFCEL*.

#### References

1. R.J. Press, K.S.V. Santhanam, M.J. Miri, A.V. Bailey and G.A. Takacs, *Introduction to Hydrogen Technology*, John Wiley&Sons, New Jersey (2009).
2. E.K. Stefanakos, D.Y. Goswami, S.S. Srinivasan and J.T. Wolan, *Hydrogen Energy*. In: M. Kutz editor, *Environmentally Conscious Alternative Energy Production*, John Wiley&Sons, New Jersey (2007).
3. U. Wittstadt, *Electrolysis: Hydrogen Production Using Electricity*. In: A. Zuttel, A. Borgschulte, L. Schlapbach editors, *Hydrogen as a Future Energy Carrier*, Wiley-VCH, Weinheim (2008).
4. M. Wang, Z. Wang, X. Gong and Z. Guo, *Renew Sust Energ Rev*, 29 (2014) 573.
5. D. Wang, Z. Wang, C. Wang, P.Zhou, Z. Wu and Z. Liu, *Electrochem Commun*, 34 (2013) 219.
6. E. Saraloğlu Güler, E. Konca and I. Karakaya, *Int. J. Electrochem. Sci.*, 8 (2013) 5496.
7. M. Smiljanić, I. Srejić, B. Grgurb, Z. Rakočević and S. Štrbac, *Electrochim Acta*, 88 (2013) 589.
8. B. Pierozynski and I.M. Kowalski, *Int. J. Electrochem. Sci.*, 8 (2013) 7938.
9. S. Trasatti, *Electrocatalysis of Hydrogen Evolution: Progress in Cathode Activation*, In: H. Gerischer and C.W. Tobias editors, *Advances of Electrochemical Science and Engineering*, VCH Verlagsgesellschaft, Weinheim (1992).
10. C. Hu, J.K. Pulleri, S.W. Ting and K.Y. Chan, *Int J Hydrogen Energy*, 39 (2014) 381.
11. D.M.F. Santos, C.A.C. Sequeira, D. Maccio, A. Saccone and J.L. Figueiredo, *Int J Hydrogen Energy*, 38 (2013) 3137.
12. C. Lupi, A. Dell'Era and M. Pasquali, *Int J Hydrogen Energy*, 39 (2014) 1932.
13. D.A.D. Corte, C. Torres, P.S. Correa, E.S. Rieder and C.F. Malfatti, *Int J Hydrogen Energy*, 37 (2012) 3025.

14. M.P.M. Kaninski, M.M. Seovic, S.M. Miulovic, D.L. Zugic, G.S. Tasic GS and D.P. Saponjic, *Int J Hydrogen Energy*, 38 (2013) 1758.
15. A. Kellenberger, N. Vaszilcsin, W. Brandl, N. Duteanu, *Int J Hydrogen Energy*, 32 (2007) 3258.
16. M.A. Dominguez-Crespo, E. Ramirez-Meneses, A.M. Torres-Huerta, V. Garibay-Febles and K. Philippot, *Int J Hydrogen Energy*, 37 (2012) 4798.
17. R. Subbaraman, D. Tripkovic, D. Strmcnik, K.C. Chang, M. Uchimura, A.P. Paulikas, V. Stamenkovic and N.M. Markovic, *Science* 334 (2011) 1256.
18. R. Solmaz and G. Kardas, *Int J Hydrogen Energy*, 36 (2011) 12079.
19. A.N. Frumkin, *Hydrogen overvoltage and adsorption mercury*, In: P. Delahay and C.W. Tobias Editors, *Advances in Electrochemistry and Electrochemical Engineering*, Interscience Publishers Inc, New York (1963).
20. M. Stackelberg and H. Fassbender, *Z Elektrochem*, 62 (1958) 834.
21. M. Stackelberg, W. Hans and W. Jensch, *Z Elektrochem*, 62 (1958) 839.
22. S.G. Mairanovskii, *Russ Chem Rev*, 33 (1964) 38.
23. Y.M. Temerk and B. Nygard, *Monatsh Chem* 109 (1978) 73.
24. G.A. Tedoradze and D.I. Dzhpapridze, *Phys Chem*, 3 (1963) 402.
25. C.C. Văduva, N. Vaszilcsin, A. Kellenberger and M. Medeleanu, *Int J Hydrogen Energy*, 36 (2011) 6994.
26. R. Cretu, A. Kellenberger and N. Vaszilcsin, *Int J Hydrogen Energy*, 38 (2013) 11685.
27. S. Trasatti, *J Electroanal Chem*, 39 (1972) 163.
28. M.J. Frisch, G.W. Trucks, H.B. Schlegel, G.E. Scuseria, M.A. Robb, J.R. Cheeseman, G. Scalmani, et al, Gaussian 09, Revision B.01 Gaussian, Inc, Wallingford CT, (2010).
29. D. Ciubotariu, M. Medeleanu, I. Iorga, E. Deretey, C. Bologa and S. Mureșan, *Chem Bull Tech Univ Timișoara*, 38 (1993) 83.
30. A.K. Khanova and L.I. Krishtalik, *J Electroanal Chem*, 660 (2011) 224.
31. C.H. Hamann, A. Hammett and W. Vielstich, *Electrochemistry*, Wiley VCH, Verlag, Weinheim (2007).
32. J. O'M. Bockris, A.K.N. Reddy and M. Gamboa-Aldeco, *Modern Electrochemistry*, Vol. 2A, Second edition, Kluwer Academic/Plenum Publishers, New York (2000).
33. D. Dobos, *Electrochemical data*, Elsevier Scientific Publishing Company, Amsterdam - Oxford - New York (1975).
34. [www.zirchrom.com/organic.htm](http://www.zirchrom.com/organic.htm).